Caffeic acid phenylethyl ester and MG132, two novel nonconventional chemotherapeutic agents, induce apoptosis of human leukemic cells by disrupting mitochondrial function

Victoria Cavaliere, Daniela L. Papademetrio, Tomás Lombardo, Susana N. Costantino, Guillermo A. Blanco & Elida M. C. Álvarez

Targeted Oncology

ISSN 1776-2596

Targ Oncol
DOI 10.1007/s11523-013-0256-y

Springer

Targ Oncol
DOI 10.1007/s11523-013-0256-y

ORIGINAL RESEARCH

Caffeic acid phenylethyl ester and MG132, two novel nonconventional chemotherapeutic agents, induce apoptosis of human leukemic cells by disrupting mitochondrial function

Victoria Cavaliere · Daniela L. Papademetrio · Tomás Lombardo · Susana N. Costantino · Guillermo A. Blanco · Elida M. C. Álvarez

Received: 24 August 2012 / Accepted: 4 January 2013

Abstract The ability to modulate balance between cell survival and death is recognized for its great therapeutic potential. Therefore, research continues to focus on elucidation of cell machinery and signaling pathways that control cell proliferation and apoptosis. Conventional chemotherapeutic agents often have a cytostatic effect over tumor cells. New natural or synthetic chemotherapeutic agents have a wider spectrum of interesting antitumor activities that merit in-depth studies. In the present work, we aimed at characterizing the molecular mechanism leading to induction of cell death upon treatment of the lymphoblastoid cell line PL104 with caffeic acid phenylethyl ester (CAPE), MG132 and two conventional chemotherapeutic agents, doxorubicine (DOX) and vincristine (VCR). Our results showed several apoptotic hallmarks such as phosphatidylserine (PS) exposure on the outer leaflet of the cell membrane, nuclear fragmentation, and increase sub-G1 DNA content after all treatments. In addition, all four drugs downregulated survivin expression. CAPE and both chemotherapeutic agents reduced Bcl-2, while only CAPE and MG132 significantly increased Bax level. CAPE and VCR treatment induced the collapse of mitochondrial membrane potential ($\Delta\psi m$). All compounds induced cytochrome *c* release from mitochondrial compartment to cytosol. However, only MG132 caused the translocation of Smac/DIABLO. Except for VCR treatment, all other drugs increased reactive oxygen species (ROS) production level. All treatments induced activation of caspases 3/7, but only CAPE and MG132 led to the activation of caspase 9. In conclusion, our results indicate that CAPE and MG132 treatment of PL104 cells induced apoptosis through the mitochondrial intrinsic pathway, whereas the apoptotic mechanism induced by DOX and VCR may proceed through the extrinsic pathway.

Keywords Apoptosis · Caffeic acid phenylethyl ester (CAPE) · MG132 · Mitochondria · Leukemia

Abbreviations

CAPE	Caffeic acid phenylethyl ester
DOX	Doxorubicine
VCR	Vincristine
DMSO	Dimethylsulfoxide
FCS	Fetal calf serum
PI	Propidium iodide
DAPI	4′-6-Diamidino-2-phenylindole
$\Delta\psi m$	Mitochondrial membrane potential
ROS	Reactive oxygen species
H_2O_2	Hydrogen peroxide
AO	Acridine orange

Victoria Cavaliere, Daniela Papademetrio and Tomás Lombardo are fellows from CONICET.
Guillermo Blanco and Elida Álvarez are members of the National Research Career CONICET.

V. Cavaliere (✉) · D. L. Papademetrio · S. N. Costantino · E. M. C. Álvarez
Laboratorio de Inmunología Tumoral (LIT), IDEHU-CONICET, Facultad de Farmacia y Bioquímica, Universidad de Buenos Aires (UBA), Buenos Aires, Argentina
e-mail: vcavaliere@ffyb.uba.ar

T. Lombardo · G. A. Blanco
Laboratorio de Immunotoxicologia (LaITO), IDEHU-CONICET, Hospital de Clínicas, José de San Martín, Universidad de Buenos Aires (UBA), Buenos Aires, Argentina

Published online: 22 February 2013

EB	Ethidium bromide
IAP	Inhibitory apoptotic proteins
MMP	Mitochondrial membrane permeabilization
XIAP	X-linked inhibitor of apoptosis
cIAP-1	Cellular inhibitor of apoptosis protein 1
cIAP-2	Cellular inhibitor of apoptosis protein 2
AML	Acute myeloid leukemia
ALL	Acute lymphoblastic leukemia
CML	Chronic myeloid leukemia
CLL	Chronic lymphoblastic leukemia

Introduction

Successful treatment of cancer is one of the greatest challenges of modern medicine. Several studies have shown that apoptosis, the most common and well-defined form of programed cell death, is one of the main causes of tumor cell death after radiotherapy and chemotherapy treatment of hematological malignancies [1–3]. Therefore, induction of apoptosis represents an efficient strategy for cancer chemotherapy and constitutes a reliable marker to evaluate and design new chemotherapeutic agents aiming at improving patient treatment outcome [4].

Apoptosis can be induced under stress conditions, exposure to cytotoxic drugs, or loss of normal adhesion to extracellular matrix [5–7]. There are distinct subtypes of apoptosis that, although morphologically similar, can be triggered through different biochemical routes.

The major and best-characterized pathways leading to apoptotic cell death are intrinsic and extrinsic ones. In the intrinsic apoptotic pathway, death-promoting stimuli converge to mitochondria favoring its dysfunction and consequent release of proapoptotic factors, in part, responsible for massive cell destruction [8].

Caffeic acid phenylethyl ester (CAPE), a derivative of caffeic acid, is a biologically active polyphenolic compound of propolis from honeybee hives and also a popular folk medicine. CAPE exhibits a broad spectrum of activities including antibacterial, antiinflammatory, antiviral, antifungal, and antitumoral properties, among others [9–12]. CAPE has been shown to induce apoptotic cell death in a variety of solid tumors [13–15]. However, little is known about the effects of CAPE in the treatment of hematological malignancies.

It has been reported that CAPE is cytotoxic to tumor cells, at least in part, due to inhibition of NF-κB signaling pathway [16, 17]. Nonetheless, a plethora of CAPE biological activities is most probably associated to alteration of more than one intracellular pathway leading to a complex and still unclear mechanism of action.

Proteasome is a large catalytic complex responsible for most nonlysosomal intracellular protein degradation. This organelle is a promising target for cancer therapy as it has been shown to impact cell cycle progression, induction of apoptosis, cell proliferation, and other physiological processes by regulating levels of important signaling proteins [18]. Therefore, proteasome inhibitors are becoming potential therapeutic agents for various types of human cancers that are refractory to current therapies.

MG132 (Z-Leu-Leu-Leu-aldehyde) is a cell-permeable tripeptide aldehyde proteasome inhibitor, which also inhibits calpains and cathepsins [19]. MG132, at low concentrations, caused significant apoptotic cell death in two malignant mesotelioma cell lines, and in this case, mitochondrial-dependent caspase activation was the underlying mechanism of action [18]. Proteasome inhibition caused by exposure to MG132 selectively induced endoplasmic reticulum dysfunction and caspase-independent cell death in human cholangiocarcinoma cells [20]. These data strongly suggest that the mechanisms of cell death by proteasome inhibition are complex and likely to be cell type specific. Thus, it is important to identify particular death pathways involved in a specific type of tumor to broaden the clinical application of proteasome inhibitors.

We have previously reported that CAPE and MG132 exert a potent and highly selective cytotoxic effect mediated by cell cycle deregulation, reduction of proliferation rate, and induction of apoptotic morphology on a novel lymphoblastoid B cell line (PL104) as well as on primary human leukemic cells. By contrast, doxorubicine (DOX) and vincristine (VCR), two conventional chemotherapeutic drugs used in treatment of hematological malignancies, showed antiproliferative rather than cytotoxic effect on PL104 cells [16].

In the present study, we aimed at exploring the underlying molecular mechanism leading to CAPE, MG132, DOX, and VCR cell death induction upon treatment of the PL104 cell line. Our results showed that all four drugs induced apoptotic cell death by differential modulation of Bcl-2 family protein members and survivin, mitochondrial dysfunction (mitochondrial membrane potential ($\Delta\psi m$) dissipation, cytochrome *c*, and Smac/DIABLO release to cytosol and increased reactive oxygen species (ROS) production), and caspase activation.

Materials and methods

Materials

CAPE and MG132 were obtained from Calbiochem (San Diego, CA, USA). Stock solutions were prepared in dimethylsulfoxide (DMSO) at 350 mM and 5 mM concentrations, respectively. VCR was kindly provided by Filaxis (Buenos Aires, Argentina) and DOX by Gador (Buenos Aires, Argentina). RPMI-1640, penicillin, and streptomycin were purchased from Invitrogen (Buenos Aires, Argentina).

Antibodies against Bcl-2, Bax, survivin, poly ADP ribose polymerase (PARP), procaspase 3, apoptosis-inducing factor (AIF), cytochrome *c*, Smac/DIABLO, β-actin, horseradish peroxidase-labeled anti-rabbit, and anti-goat secondary antibodies were purchased from Santa Cruz Biotechnology, Inc. (Buenos Aires, Argentina).

Cell lines and culture conditions

PL104 cells correspond to a lymphoblastoid cell line established in our laboratory as previously described [16]. Cell suspensions were cultured at 37 °C in a 5 % CO_2 atmosphere using RPMI-1640 medium supplemented with 15 % heat-inactivated fetal calf serum (FCS), 2 mM L-glutamine, 20 mM HEPES buffer, 100 mg/ml penicillin, 150 mg/ml streptomycin, and 50 mM 2-mercaptoethanol. Cells were subcultured at 1:2 to 1:4 ratios every 2 to 3 days with viability greater than 90 % (assessed by trypan blue). Treated cells were exposed to CAPE (0–360 μM), MG132 (0–4 μM), DOX (0–2 μM), or VCR (0–5 μM) during 2 to 24 h according to the parameter being evaluated. Control cells were treated with RPMI-1640 FCS 15 % or DMSO 0.1 % v/v.

Collection of cells from leukemia patients and healthy donors

Patient-derived leukemic (PDL) cells were obtained, after informed consent and in accordance with the Declaration of Helsinki, from bone marrow aspirates. Samples from 20 nontreated patients at diagnosis, immunophenotypically characterized as acute myeloid leukemia [n=8], acute lymphoblastic leukemia [n=7], chronic lymphoblastic leukemia [n=3], and chronic myeloid leukemia [n=2], were analyzed. Patients were 16 males and four females, and the mean age was 61.6±23.1 years (range, 3–63 years). Patients under treatment or relapse phase were excluded.

Normal peripheral blood samples were obtained from eight healthy volunteers after informed consent. The male-to-female ratio was 5:5 with a mean age of 35 years (range, 23–60 years).

PDL cells from bone marrow aspirates or normal peripheral blood mononuclear cells (PBMC) were isolated by Ficoll-Hypaque density gradient centrifugation and cultured in RPMI-1640 containing 20 % FCS at 37 °C in a humidified atmosphere with 5 % CO2. In all cases, cell viability was greater than 95 %, as assessed by trypan blue exclusion.

Annexin V assay

Exposed phosphatidylserine (PS) on cell surface was determined by staining with annexin V–FITC/propidium iodide (PI; Apoptosis Detection Kit; BioVision, Inc., Mountain View, CA, USA) assay. Briefly, 1×10^6 PL104 cells/ml were treated with CAPE (180 and 360 μM), MG132 (2 and 4 μM), DOX (1.5 and 2 μM), and VCR (1 and 5 μM) for 24 h. Single-cell suspensions were analyzed in a FACSCalibur flow cytometer (Becton Dickinson, San Jose, CA, USA) and data were analyzed using WinMDI 2.9 software (Scripps Institute, La Jolla, CA, USA).

TUNEL assay

To detect the characteristic DNA fragmentation of apoptosis at single-cell level, PL104 cells were either exposed to CAPE (180 μM), MG132 (2 μM), DOX (1.5 μM), or VCR (1 μM) during 24 h or pretreated with pancaspase inhibitor, Z-VAD.fmk (100 μM), for 2 h. Terminal deoxynucleotidyl transferase (rTdT)-mediated dUTP nick-end labeling (TUNEL) staining was performed following the manufacturer's instructions provided in DeadEnd™ Fluorometric TUNEL System detection kit (Promega, Argentina). The positive control corresponded to PL104 cells treated with 10 U/ml of DNAse I. The negative control was a similar sample run without rTdT enzyme. Slides were visualized by fluorescence microscopy (Olympus BX51; Olympus, Center Valley, PA, USA). A minimum of 200 cells were counted for each condition. Positive cells were scored as those with pyknotic nucleus and dark green fluorescent staining. The percentage of positive cells was calculated as follows:

$$\%\ \text{positive cells} = (\text{number of green fluorescent cells}/\text{number of blue fluorescent} - \text{DAPI stained} - \text{cells}) \times 100.$$

Detection of hypodiploid cells by flow cytometry

Sub-G1 DNA content in CAPE-, MG132-, DOX-, and VCR-treated cells was measured by flow cytometry. Briefly, 1×10^6 cells/ml were harvested, washed once with ice-cold phosphate buffered saline buffer (PBS), and fixed with 1 ml of ice-cold 70 % ethanol at 4 °C for 30 min. Next, PL104 cells were suspended in 1 ml of hypodiploid solution containing 1 μg/ml of 4′-6-diamidino-2-phenylindole (DAPI; Roche S.A., Buenos Aires, Argentina)–0.1 % Triton X-100 and finally, incubated for 30 min at room temperature [21]. Cellular DNA content was measured using a PAS III flow cytometer (Partec, Görlitz, Germany). Fifteen thousand events were acquired for each sample. Results were analyzed using WinMDI 2.9 software (Scripps Institute, La Jolla, CA, USA). The apoptotic population corresponded to the percentage of cells with sub-G1 DNA content.

Preparation of nuclear and cytoplasmic extracts

Nuclear extracts were prepared as previously described [22]. Briefly, treated cells were incubated in 400 μl of hypotonic buffer (10 mM HEPES pH 7.9, 1.5 mM MgCl2, 10 mM KCl, 0.5 mM dithiothreitol (DTT), 0.5 mM phenylmethanesulfonylfluoride (PMSF), 0.1 % Nonidet P-40) for 15 min on ice

and centrifuged at 11,000*g* for 10 min. Nuclear pellets were suspended in 60 μl of nuclear lysis buffer (20 mM HEPES, 1.5 mM MgCl2, 420 mM NaCl, 0.5 mM DTT, 0.5 mM PMSF, 0.2 mM ethylenendiaminetetraacetic acid (EDTA), 25 % glycerol) and incubated at 4 °C for 15 min followed by centrifugation at 13,000*g* for 15 min. Finally, the supernatants corresponding to nuclear extracts were stored at −70 °C until further use. For cytoplasmic extract preparation, cells were lysed with a hypotonic buffer (20 mM Tris pH 8.0, 150 mM NaCl, 100 mM NaF, 10 % glycerol, 1 % Nonidet P-40, 1 mM PMSF, 40 μg/ml leupeptin, and 20 μg/ml aprotinin) for 25 min at 4 °C and centrifuged at 12,000*g* for 30 min. The supernatants were stored at −70 °C and protein concentration was determined by Bradford assay.

Preparation of cytoplasmic extracts for cytochrome *c* and Smac/DIABLO detection

PL104 cells were cultured during 2, 6, 15, or 24 h with CAPE, MG132, DOX, or VCR at previously established concentrations. Briefly, cells were washed twice with ice-cold PBS, pH 7.4, followed by centrifugation at 200*g* for 5 min; the pellet was suspended in 600 μl extraction buffer containing 200 mM mannitol, 68 sucrose, 50 mM HEPES, pH 7.4, 50 mM KCl, 5 mM ethylene glycol tetraacetic acid (EGTA), 2 mM MgCl2, 1 mM dithiothreitol and protease inhibitors (1 μg/ml pepstatin, 1 μg/ml, 1 μg/ml leupeptin, 0.4 mM PMSF, 1 μg/ml aprotinin). Extracts were incubated for 30 min on ice, sonicated, and centrifuged at 14,000*g* for 15 min. Supernatants were removed and stored at −70 °C and protein concentration was determined by Bradford assay [23].

Western blot analysis

Equal amounts of protein extracts (50 μg/lane) were resolved by SDS-polyacrylamide gel electrophoresis and transferred onto a nitrocellulose membrane (Sigma-Aldrich). The membrane was blocked overnight at 4 °C in Tris-buffered saline, containing 2 % glycine and 3 % nonfat dried milk. In a next step, the membrane was incubated with specific antibodies to Bcl-2, Bax, survivin, PARP, procaspase 3, AIF, Smac/DIABLO, cytochrome *c*, and β-actin for 2 h at 37 °C followed by incubation with horseradish peroxidase-labeled secondary antibody for 1.5 h at 37 °C. The reaction was developed using a chemiluminescence detection system (Santa Cruz Biotechnology, Inc., Buenos Aires, Argentina). Densitometric analysis was performed using Scion Image software (Scion Corporation, NIH, Bethesda, MD, USA). Densitometric index and cleavage index were calculated as follows:

$$\text{Densitometric index} = \text{OD treatment}/\text{OD control}$$

$$\text{Cleavage index} = (\text{OD cleaved fragment}/\text{OD total})\ \text{treatment}/(\text{OD cleaved fragment}/\text{OD total})\ \text{control}.$$

Measurement of Δψm by flow cytometry

Changes in the inner mitochondrial transmembrane potential were determined with the potentiometric cationic lypophilic probes TMRE and $DiOC6_{(3)}$ (Molecular Probes, Argentina) by incubating 1×10^6 treated cells for 20 min at 37 °C in the presence of TMRE 0.05 μM (for CAPE, MG132, and VCR treatments) or $DiOC6_{(3)}$ 0.01 μM (for DOX treatment). In all cases, a positive control was obtained by exposing a sample of cells to the mitochondrial uncoupling agent CCCP (50 μM). After loading the cells with the probes, they were washed once with PBS and analyzed in a PAS III flow cytometer (Partec, Görlitz, Germany). Fifteen thousand events were acquired for each sample. The data were analyzed using WinMDI 2.9 software (Scripps Research Institute, La Jolla, CA, USA). The fraction of cells with low Δψm was scored as the percentage of cells with low fluorescence intensity.

Assessment of intracellular ROS production by flow cytometry

ROS level was monitored using the fluorescent probes dichlorodihydrofluorescein diacetate (H_2DCF-DA) and hydroethidine (HE) (Sigma-Aldrich, Argentina). H_2DCF-DA is a stable nonpolar compound that readily diffuses into cells and is hydrolyzed by intracellular esterase to yield DCHF, which is retained within the cells. Hydrogen peroxide (H_2O_2) or low molecular weight peroxides produced by the cells oxidize DCHF to the highly fluorescent compound 2′,7′-dichlorofluorescein (DCF). Thus, fluorescence intensity is proportional to the amount of H_2O_2 produced by the cells. HE was used as a fluorescent probe for intracellular superoxide anion production. PL104 cells were cultured in the presence of CAPE (0–360 μM), MG132 (0–4 μM), DOX (0–2 μM), and VCR (0–5 μM) during 6, 15, or 24 h. Afterwards, cells were loaded with either 1 μM H_2DCF-DA or 2 μM HE for 30 min at 37 °C. Positive controls were obtained by exposing a sample of cells to 100 μM H_2O_2 for 30 min (H_2DCF-DA assay) or 50 μM menadione (Sigma-Aldrich, Argentina) for 24 h (HE assay) before staining with the probes. Cells were finally examined in a PAS III flow cytometer (Partec, Görlitz, Germany). Fifteen thousand events were acquired for each sample. The data were analyzed using WinMDI 2.9 software (Scripps Research Institute, La Jolla, CA, USA).

Analysis of caspase activity

Cells (1.5×10^4) per well were treated with CAPE (180 μM), MG132 (2 μM), DOX (1.5 μM), or VCR (1 μM), either

with or without pretreatment with pancaspase inhibitor, Z-VAD.fmk (100 μM), during 6, 15, and 24 h. The activity of caspase 3/7 and 9 was determined following the manufacturer's instructions provided in Caspase-Glow® 3/7 and Caspase-Glow® 9 detection kit (Promega, Argentina). Luminescence production was measured on a Victor plate-reading luminometer (PerkinElmer). The signal obtained was proportional to caspase 3/7 or 9 activity in cell culture. Caspase activity in samples was scored as activity index that was calculated as follows:

$$\text{Activity index} = \text{luminescence units of treated cells} / \text{luminescence units of control cells.}$$

Acridine orange and ethidium bromide staining

Morphological features associated with apoptosis were analyzed by acridine orange (AO) and ethidium bromide (EB) staining after pretreatment of PL104 cells with Z-VAD.fmk (100 μM) followed by the exposure to 180 μM CAPE, 2 μM MG132, 1.5 μM DOX, and 1 μM VCR for 24 h more. Briefly, cells were suspended in a dye mix (100 μg/ml AO plus 100 μg/ml EB in PBS) and visualized by fluorescence microscopy (Carl Zeiss, Germany) [16]. A minimum number of 200 cells were analyzed for each condition, and apoptotic cells were scored as the number of cells with fragmented nuclei, enlarged cytoplasm, and condensed chromatin. The percentage of apoptotic cells was calculated as follows:

$$\%\ \text{apoptotic cells} = (\text{number of cells with apoptotic nuclei} / \text{total number of cells counted}) \times 100.$$

Statistical analysis

All data are presented as mean+SD of a series of three independent experiments. Statistical analyses were performed with Prism 3 software (GraphPad, San Diego, CA, USA) using one-way analysis of variance followed by Tukey's post hoc comparison test. Group differences, treated versus untreated, were considered statistically significant when $p<0.05$.

Results

CAPE, MG132, DOX, and VCR cause exposure of PS on cell surface and induce nuclear apoptotic hallmarks in PL104 cells

In our previous work, we have shown that treatment of PL104 cells with different concentrations of CAPE and MG132 resulted in high percentages of cells with apoptotic morphology. In the present study, we analyzed PS exposure on drug-treated PL104 cells by labeling with fluorescent annexin V. Figure 1a shows that treatment with CAPE (180 and 360 μM), MG132 (2 and 4 μM), DOX (1.5 and 2 μM), and VCR (1 and 5 μM) caused the exposure of PS in the outer leaflet of cell membrane in all assays conducted at 24 h. The percentage of annexin V-positive cells increased with higher concentrations of CAPE, MG132, and DOX.

We further evaluated the effect of CAPE, MG132, DOX, and VCR on PL104 cells on DNA content and nuclear fragmentation. Figure 1b shows an increase in the percentage of cells having DNA fragmentation after 24-h treatment with CAPE (180 and 360 μM), MG132 (2 and 4 μM), DOX (0.5, 1.5, and 2 μM), and VCR (1 and 5 μM). The same treatments considerably increased the number of cells with sub-G1 DNA content at 24 h (Fig. 1c). These data, together with the previously described morphologic and biochemical changes, confirm the occurrence of apoptosis.

CAPE, MG132, DOX, and VCR differentially modify the expression of key apoptotic regulatory proteins in PL104 cells

Bcl-2 and IAP families of proteins play a pivotal role in apoptotic program regulation. Therefore, we investigated the contribution of Bax, Bcl-2, and survivin to apoptotic cell death induced by CAPE, MG132, DOX, and VCR in PL104 cells. CAPE (180 μM) considerably reduced Bcl-2 expression after 6 and 15 h of exposure (Fig. 2a, d). By contrast, MG132 did not alter Bcl-2 expression level at any of the experimental conditions tested (Fig. 2a, d). The proapoptotic protein Bax was upregulated to a large extent after 15 h of treatment with CAPE or MG132. DOX (1.5 μM) and VCR (1 μM) decreased Bcl-2 expression that was detected only at 6-h post-treatment (Fig. 2a, d), but they did not induce major changes in Bax expression (Fig. 2b, d).

CAPE strongly decreased survivin protein level at early time points (6 h and 15 h), while MG132, DOX, and VCR showed a similar effect that was clearly observed after 24 h (Fig. 2c, d). These results suggest that CAPE downregulates antiapoptotic protein expression (Bcl-2 and survivin) in an early phase followed by a late increase in Bax expression that contributes to the initiation of apoptosis. MG132 upregulates Bax level but also decreases survivin, while DOX and VCR only alter the expression of Bcl-2 and survivin.

CAPE and VCR treatment, but not MG132 or DOX, decrease Δψm in PL104 cells

Loss of Δψm is often associated with alteration of inner mitochondrial membrane and is one of several events that characterize mitochondrial membrane permeabilization (MMP). We measure Δψm in treated cells by flow cytometry using the sensitive Δψm probes TMRE or $DiOC_6(3)$. A

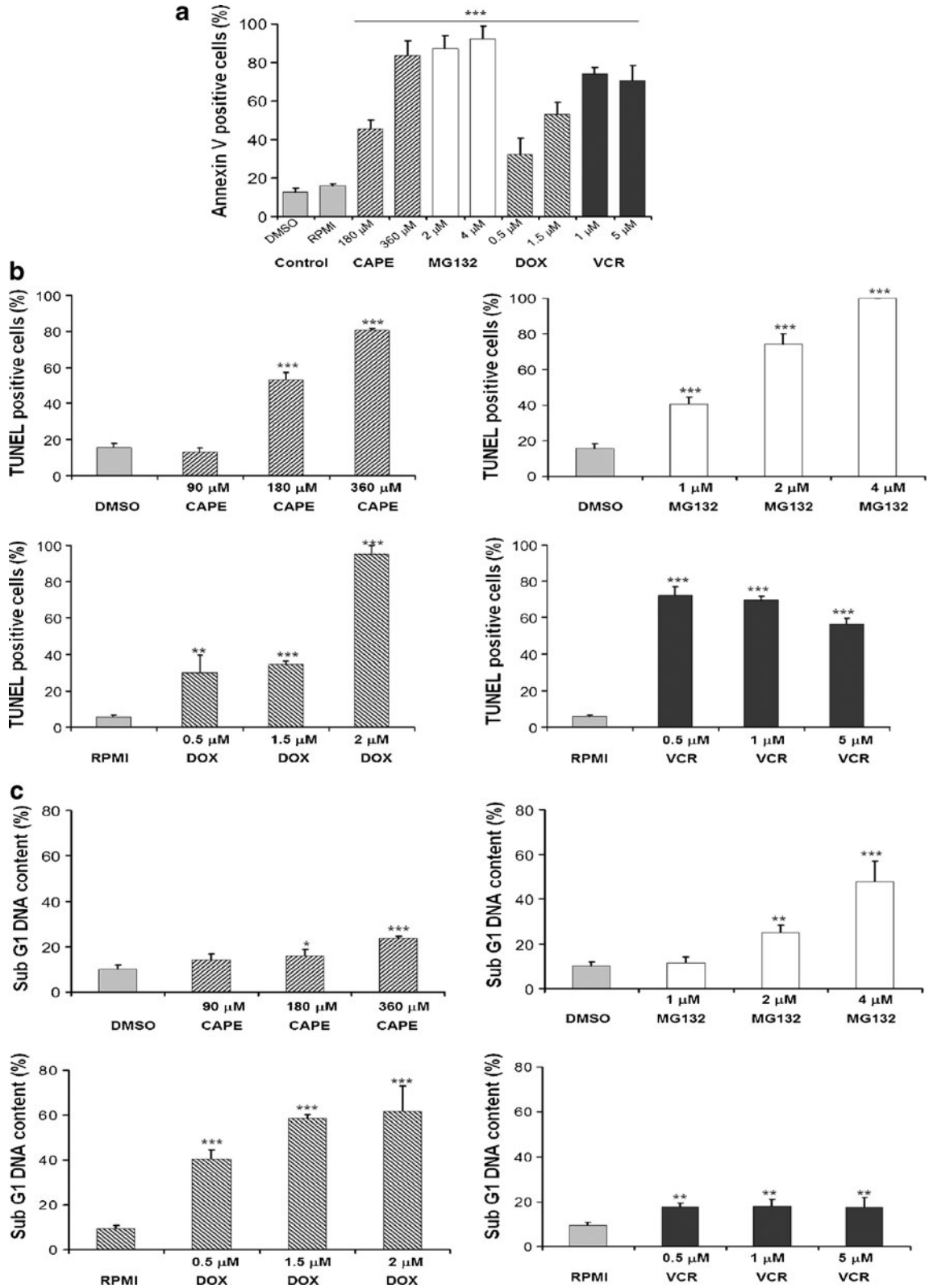

decrease of Δψm was detected at 6, 15, and 24 h after treatment of PL104 cells with 180 and 360 μM CAPE. The maximal effect was attained after 15-h treatment with 360 μM and corresponded to 90 % of cells having collapsed Δψm (Fig. 3a). VCR also induced a decrease of Δψm that did not change significantly when the dose was increased, persisted after 24-h exposure, and attained a maximal effect of about 30 % of cells having collapsed Δψm (Fig. 3d). In

◀ **Fig. 1** Phosphatidylserine expression on cell surface, DNA fragmentation, and sub-G1 DNA content analysis. **a** Labeling of cells with fluorescent annexin V. *Bar graphs* represent the percentage of positive cells after treatment with CAPE, MG132, DOX, and VCR for 24 h at the indicated doses. Control treatments correspond to DMSO 0.1 % v/v for CAPE and MG132 and RPMI for DOX and VCR. **b** TUNEL labeling of cells to quantify DNA fragmentation. *Bar graphs* represent the percentage of positive cells after treatment with CAPE, MG132, DOX, and VCR for 24 h at the indicated doses. **c** DNA content analysis to identify apoptotic cells with hypodiploid DNA content. *Bar graphs* represent the percentage of cells with sub-G1 DNA content after treatment with CAPE, MG132, DOX, and VCR for 24 h at the indicated doses. In all cases, *bars* indicate mean+SD of at least three independent experiments. Differences between the mean of treated and control cells were analyzed with Tukey's post-test after ANOVA; (*) $p<0.05$; (**) $p<0.01$; (***) $p<0.001$

contrast, MG132 and DOX did not affect Δψm even after 24-h exposure with the highest doses (Fig. 3b, c). This data indicates that CAPE and VCR adversely affect mitochondrial integrity in PL104 cells by disrupting Δψm prior to the induction of apoptotic cell death. By contrast, MG132 and DOX induce apoptosis without altering Δψm at any of the conditions tested.

CAPE, MG132, DOX, and VCR cause release of mitochondrial intermembrane proteins to the cytosol in PL104 cells

Another event that characterizes MMP is the release of mitochondrial intermembrane proapoptotic proteins to the cytosol. Thus, we examined by western blot whether CAPE, MG132, DOX, or VCR modified cytochrome *c* and Smac/DIABLO levels. Treatment with 180 μM CAPE resulted in an increase in cytochrome *c* expression at 2 and 24 h with lower levels in between these two time points (Fig. 4a, e). MG132 induced the release of cytochrome *c* from mitochondria to cytosol after 2, 15, and 24 h of treatment (Fig. 4b, e). DOX induced a first significant increase in cytochrome *c* at 6 h, and a high expression was still observed after 24 h (Fig. 4c, e). VCR treatment significantly increased the expression of cytochrome *c* at 6 and 15 h (Fig. 4d, e). MG132 increased Smac/DIABLO expression after 6-h exposure, while the rest of the drugs tested did not induce any significant changes in this protein level (Fig. 4b, e). In summary, these results indicate that induction of apoptosis by all four drugs in PL104 cells involve cytochrome *c* release from mitochondrial compartment to cytosol. However, only MG132 caused cytosolic increase of both cytochrome *c* and Smac/DIABLO.

CAPE, MG132, and DOX, but not VCR, causes an increase in ROS production in PL104 cells

Lethal stimuli often alter cellular energy metabolism to such an extent that leads to bioenergetic catastrophe where oxidative phosphorylation is arrested and ROS production is progressively increased. Thus, we evaluated ROS level on PL104 cells by flow cytometry after treatment with CAPE, MG132, DOX, and VCR. Using the fluorescent probe HE, we detected increased levels of superoxide anion after 6 and 15 h of treatment with 90, 180, and 360 μM CAPE (Fig. 5a). By contrast, MG132 did not induce a statistically significant increase in superoxide anion after 6-h incubation. A slight increase to about 20 % HE-positive cells was detected with 2 μM dose and 50 % with 4 μM dose at 15 h (Fig. 5a). VCR treatment did not modify superoxide anion levels in any of the conditions tested (Fig. 5a). CAPE also induced a marked increment in H_2O_2 production as detected by the fluorescent probe H_2DCF-DA (30 % positive cells). An increase in H_2O_2 was evident after 15 and 24 h either with 180 μM or 360 μM (Fig. 5b). Again, treatment with either MG132 or VCR did not induce any significant changes in H_2O_2 levels at 15 or 24 h (Fig. 5b). By contrast, 6-h treatment with DOX increased H_2O_2 levels to about 40 % positive cells, and this level was even increased to more than 50 % positive cells after 15 and 24 h with 2 μM and 1.5 μM dose (Fig. 5b). These observations suggest that CAPE and DOX strongly increase PL104 ROS production, while MG132 and VCR have only a mild or no effect, respectively, on intracellular ROS level.

CAPE, MG132, DOX, and VCR induce caspase activation in PL104 cells

Massive caspase activation is a common feature of apoptosis and contributes to the late morphologic changes observed in apoptotic cells. We investigated the role of caspases in apoptotic cell death of PL104 cells by analyzing protein expression of procaspase 3, PARP, and AIF. Procaspase 3 expression showed a 2.5-fold reduction after 6 and 24 h of treatment with CAPE as compared to untreated cells (Fig. 6a, b). Reduced expression of procaspase 3 was associated with an increase in PARP cleavage, in agreement with PARP being a substrate of caspase 3 (Fig. 6a, b). MG132 also decreased procaspase 3 after 6 and 15 h of treatment and increased PARP cleavage, being more evident at 24 h (Fig. 6a, c). DOX treatment resulted in a reduction of procaspase 3 expression at 6 and 24 h, with a concomitant increase in PARP cleavage at 15 and 24 h (Fig. 6a, d). No change in procaspase 3 expression was observed after VCR treatment. However, cleavage of PARP was significantly increased after 15 and 24 h (Fig. 6a, e). Expression of AIF, a caspase-independent apoptosis effector protein, was not modified by any of the four drugs at any of the several time points and doses tested (Fig. 6a). We further confirm caspase activity in response to drug treatment by a luminescent-based caspase 3/7 assay. CAPE showed more than fourfold increase in caspases 3/7 activity within 6 to 15 h of

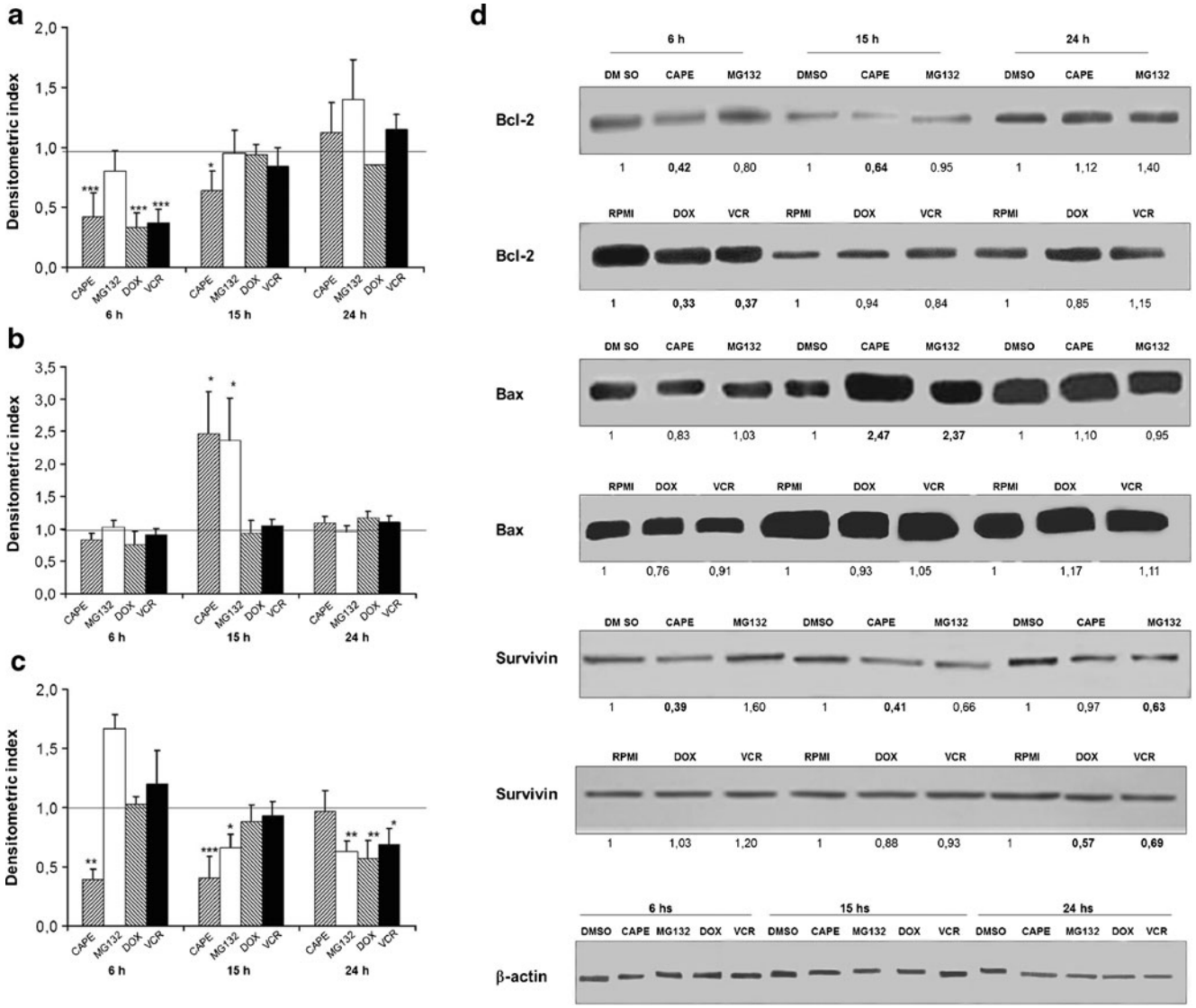

Fig. 2 Modulation of antiapoptotic proteins Bcl-2 and survivin and proapoptotic protein Bax. Cytoplasmic extracts obtained from PL104 cells treated with CAPE 180 μM, MG132 2.0 μM, DOX 1.5 μM, and VCR 1.0 μM for the indicated time periods were used to determine the relative levels of Bcl-2 (**a**), Bax (**b**), and survivin (**c**) protein expression. Densitometric index of 1.0 (*dark horizontal line*) represents the reference basal level in untreated cells. *Bars* indicate mean densitometric index+SD of at least three experiments. Differences between the mean of treated cells and the densitometric reference value of 1.0 were analyzed with Tukey's post-test after ANOVA; (*) $p<0.05$; (**) $p<0.01$; (***) $p<0.001$. **d** A representative blot image with densitometric index values. RPMI corresponds to untreated cells, and DMSO corresponds to cells treated with 0.1 % v/v DMSO in RPMI. Statistically significant densitometric index values are indicated in *bold numbers*. The level of β-actin was also measured as an internal control

treatment and a further decrease in its activity at 24 h (Fig. 7a). MG132 induced a 7.7-fold increase in caspases 3/7 activity after 6-h treatment, which decreased to about half of that value at 15 and 24 h (Fig. 7a). Both DOX and VCR induced a clear time-dependent increase in caspases 3/7 activity, with values of twofold increase at 6 h to about 4.5-fold increase at 24 h (Fig. 7a). Caspases 3/7 can be activated mainly due to caspase 8 and/or 9 activation. Because caspase 9 is specifically activated through the intrinsic apoptotic pathway, which, in turn, may be induced after various intracellular stimuli as well as cytotoxic drug exposure, we measured caspase 9 activation after treatment with CAPE, MG132, DOX, and VCR. Caspase 9 activity was considerably increased after treatment with CAPE and MG132 but not with DOX or VCR. CAPE induced a 1.5-fold increase in caspase 9 activity at 4 h (Fig. 7b). MG132 treatment resulted in an early (after 4 h) 1.5-fold increase in caspase 9. A twofold increase in caspase 9 activity was observed after 6 h of exposure, while at 15-h post-treatment, the activity index registered was similar to that

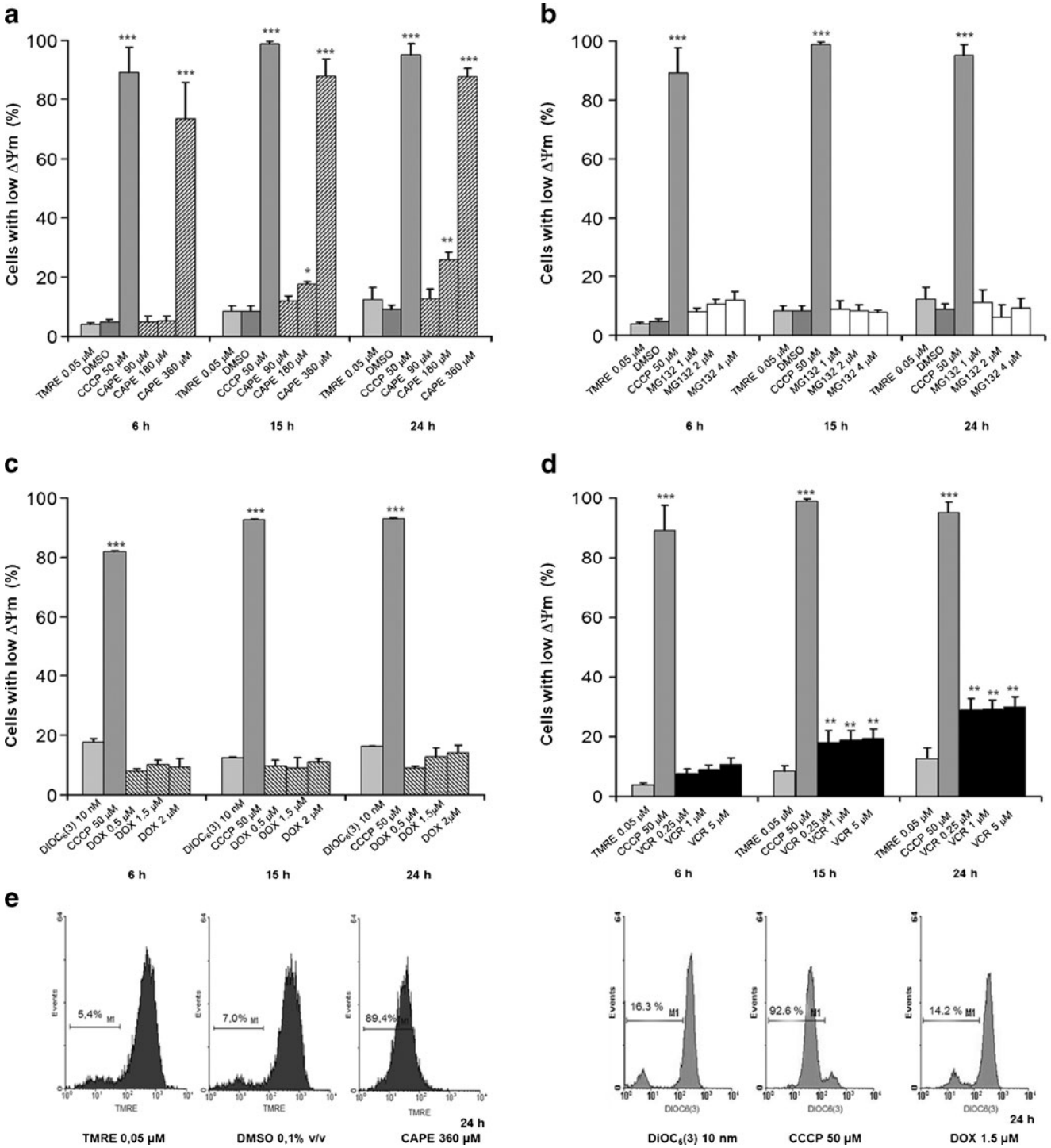

Fig. 3 Modulation of mitochondrial membrane potential. Percentage of cells with depolarized mitochondria (detected by low TMRE fluorescence) after treatment with CAPE (**a**), MG132 (**b**), DOX (**c**), and VCR (**d**) for the indicated time periods and at the indicated doses. DMSO corresponds to cells treated with 0.1 % v/v DMSO in RPMI and CCCP is a positive control of cells with depolarized mitochondria generated by uncoupling the respiratory chain. Depolarization of mitochondria caused by CAPE, MG132, and VCR was detected by staining with TMRE, while the one caused by DOX was detected by low $DIOC_6(3)$ fluorescence due to overlap of TMRE red fluorescence with DOX red fluorescence. *Bars* indicate mean+SD of at least three independent experiments. Differences between the mean of treated and control cells for each time period were analyzed with Tukey's post-test after ANOVA; (*) $p<0.05$; (**) $p<0.01$; (***) $p<0.001$. **e** Representative TMRE and $DIOC_6(3)$ fluorescence histograms of control and treated cells

of 4-h treatment. Thus, CAPE and MG132 appear to induce apoptosis on PL104 cells through a mitochondrial-dependent pathway, while DOX and VCR may do the same independently of caspase 9 activation.

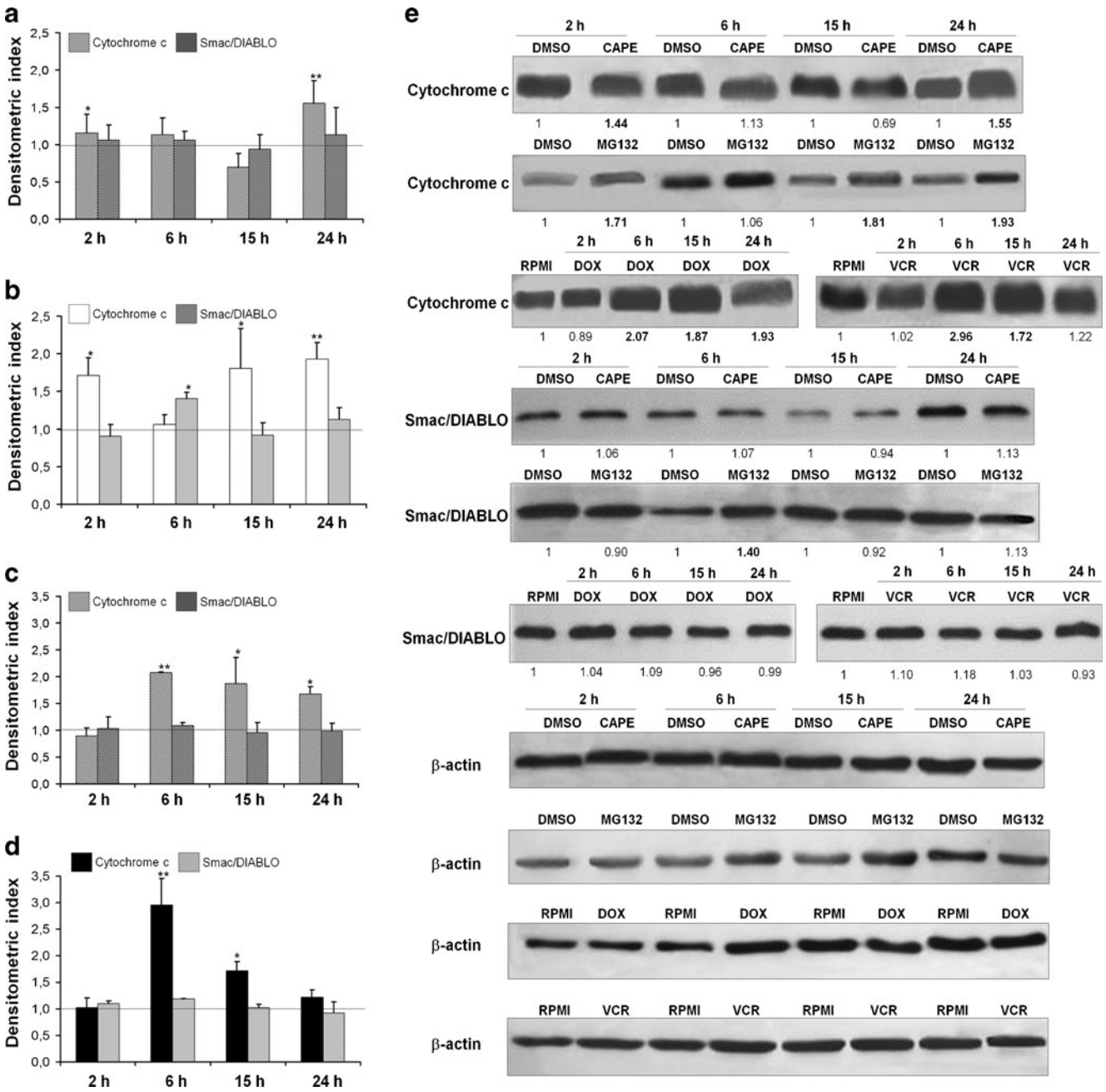

Fig. 4 Release of mitochondrial intermembrane proteins to the cytosol. Cytoplasmic extracts obtained from PL104 cells treated with CAPE 180 μM (**a**), MG132 2.0 μM (**b**), DOX 1.5 μM (**c**), and VCR 1.0 μM (**d**) for the indicated time periods were used to determine the relative levels of cytochrome *c* and Smac/DIABLO. DMSO corresponds to cells treated with 0.1 % v/v DMSO in RPMI. Densitometric index of 1.0 (*dark horizontal line*) represents the reference basal level in untreated cells. *Bars* indicate mean densitometric index+SD of at least three independent experiments. Differences between the mean of treated cells and the densitometric reference value of 1.0 were analyzed with Tukey's post-test after ANOVA; (*) $p<0.05$; (**) $p<0.01$. **e** Representative blot images for cytochrome *c*, Smac/DIABLO, and β-actin, with the corresponding densitometric index values of treated and control cells. Statistically significant densitometric index values are indicated in *bold numbers*

CAPE, MG132, DOX, and VCR-induced apoptosis is blocked by general caspase inhibitors

To conclude on the involvement of caspases in drug-induced apoptosis of PL104 cells, we tested whether or not pretreatment with the peptide Z-VAD.fmk, a pancaspase inhibitor, could block drug-induced cell death and the apoptotic phenotype. In all cases, pretreatment with Z-VAD.fmk decreased the percentage of apoptotic cells in 24-h drug-treated samples as determined by AO/EB staining (Fig. 8a). The reduction of positive cells in Z-VAD.fmk-treated samples compared to untreated cells were 78 %,

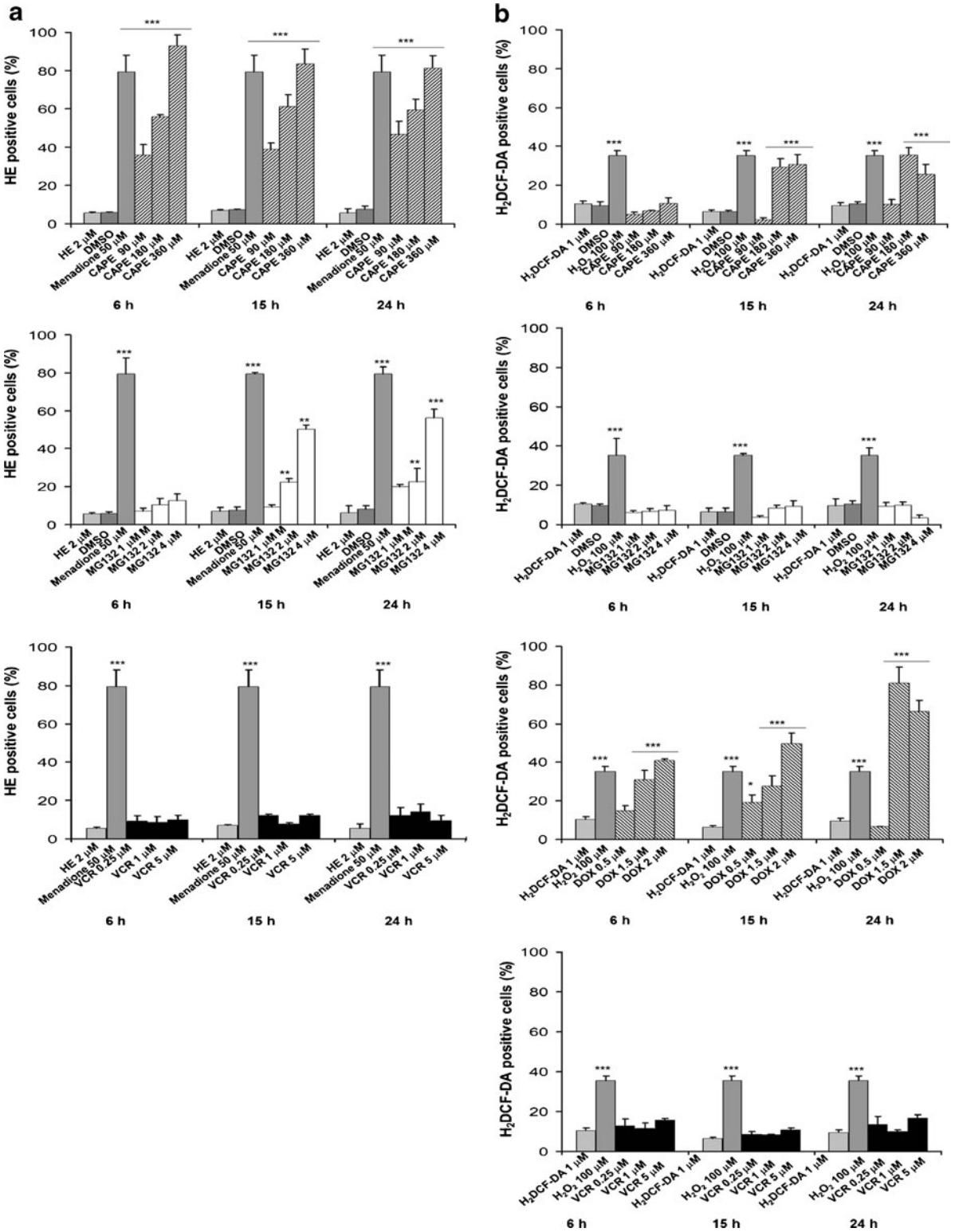

Fig. 5 ROS production. Percentage of HE-positive cells (**a**) and H_2DCF-DA-positive cells (**b**) after treatment with CAPE, MG132, DOX, and VCR for the indicated time periods and at the indicated doses. DMSO corresponds to cells treated with 0.1 % v/v DMSO in RPMI, and menadione and H_2O_2 treatments represent the corresponding positive controls for each fluorescent probe, respectively. ROS generation caused by CAPE, MG132, and VCR was detected by staining with both of HE and H_2DCF-DA fluorescent probes, while ROS caused by DOX was detected by H_2DCF-DA fluorescence due to overlap of HE red fluorescence with DOX red fluorescence. *Bars* indicate mean+SD of at least three independent experiments. Differences between the mean of treated and control cells for each time period were analyzed with Tukey's post-test after ANOVA; (*) $p<0.05$; (**) $p<0.01$; (***) $p<0.001$

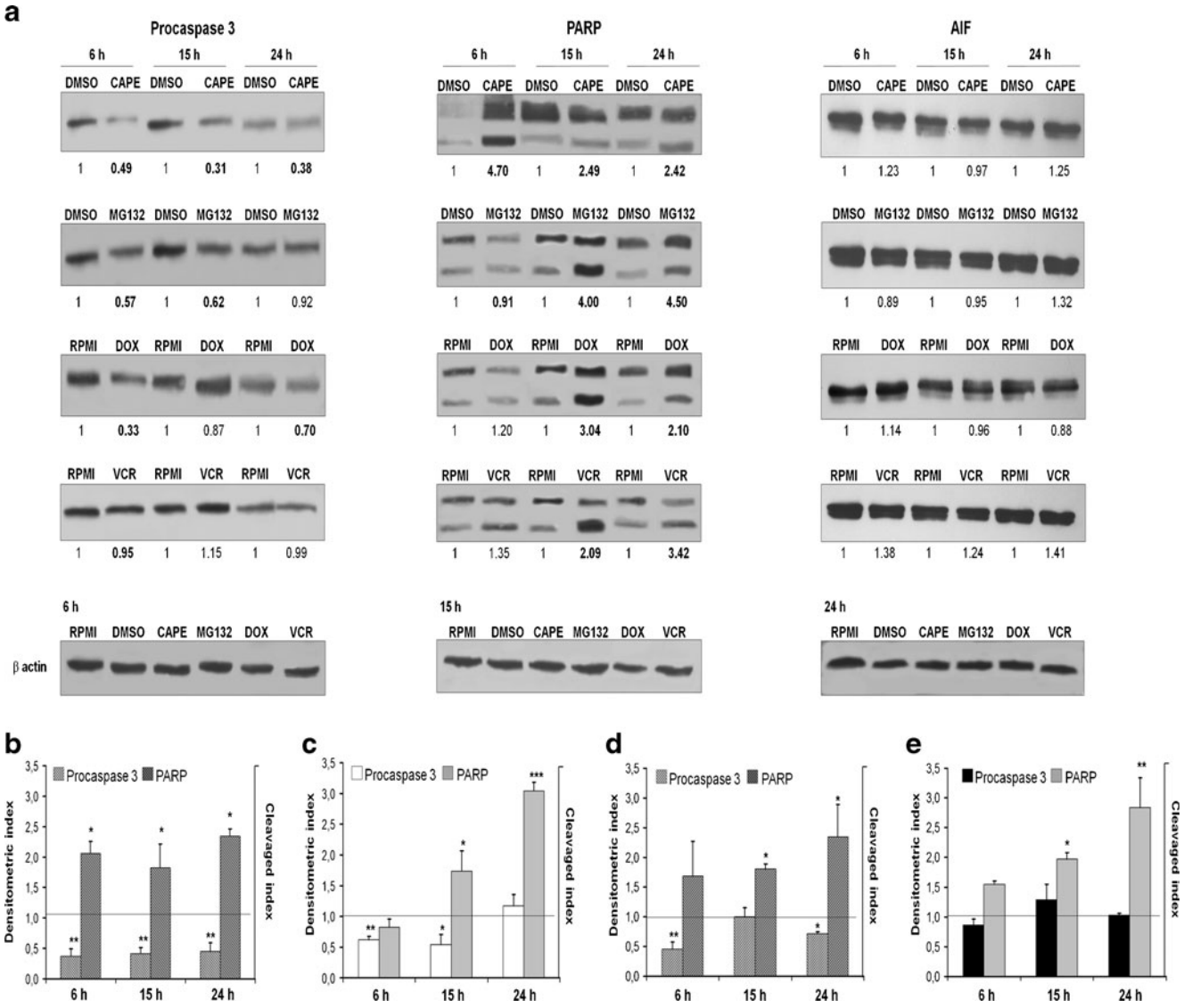

Fig. 6 Caspase activation. Cytoplasmic and nuclear extracts obtained from PL104 cells treated with 180 μM CAPE, 2.0 μM MG132, 1.5 μM DOX, and 1.0 μM VCR for the indicated time periods were used to determine the relative protein levels of procaspase 3, PARP, and AIF. DMSO corresponds to cells treated with 0.1 % v/v DMSO in RPMI. **a** Representative blot images for procaspase 3, PARP, AIF, and β-actin with the corresponding densitometric index values for procaspase 3, AIF, and β-actin or the cleavage index for PARP of treated and control cells. Statistically significant densitometric index/cleavage index values are indicated in *bold numbers*. *Bar graphs* for CAPE (**b**), MG132 (**c**), DOX (**d**), and VCR (e). Densitometric index/cleavage index of 1.0 (*dark horizontal line*) represents the reference basal level in untreated cells. *Bars* indicate mean densitometric index/cleavage index+SD of at least three independent experiments. Differences between the mean of treated cells and the index reference value of 1.0 were analyzed with Tukey's post-test after ANOVA; (*) $p<0.05$; (**) $p<0.01$; (***) $p<0.001$

80 %, 50 %, and 70 % for 180 μM CAPE, 2 μM MG132, 1.5 μM DOX, and 5 μM VCR, respectively. We further confirm this blocking effect of Z-VAD.fmk by quantifying drug-induced DNA fragmentation by TUNEL assay, procaspase 3 expression, PARP cleavage, and caspase 3/7 activity. The percentage of TUNEL-positive cells induced by treatment with CAPE, MG132, DOX, and VCR was significantly reduced after pretreatment with Z-VAD.fmk (Fig. 8b). Analysis of procaspase 3 expression through western blot showed an increase for Z-VAD.fmk+CAPE and Z-VAD.fmk+DOX compared to CAPE and DOX treatments alone (Fig. 8c). As noted above, no modulation of procaspase 3 expression was observed after 24-h treatment with MG132 or VCR, and accordingly, no increment of procaspase 3 was observed with Z-VAD.fmk pretreatment (Fig. 8c). Finally, in all cases, pretreatment with Z-VAD.fmk decreased PARP cleavage (Fig. 8c) and resulted in approximately 100 % decrease of caspase 3/7 activity (Fig. 8d). Altogether, these blocking effects of Z-VAD.fmk, with the aforementioned lack of AIF

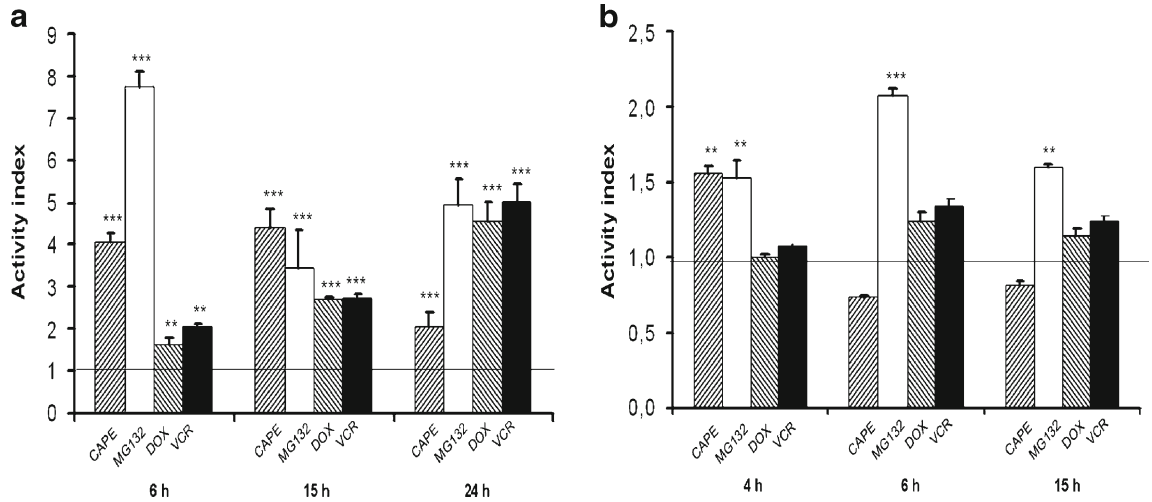

Fig. 7 Caspases 3/7 and 9 activity. PL104 cells treated with 180 μM CAPE, 2.0 μM MG132, 1.5 μM DOX, and 1.0 μM VCR for the indicated time periods were used to determine the activity of caspases 3/7 (**a**) and caspase 9 (**b**) by means of a luminescence-based detection kit following the manufacturer's instructions. Activity index of 1.0 (*dark horizontal line*) represents the reference basal level in untreated cells. *Bars* indicate mean activity index+SD of at least three independent experiments. Differences between the mean of treated cells and the index reference value of 1.0 were analyzed with Tukey's post-test after ANOVA; (*) $p<0.05$; (**) $p<0.01$; (***) $p<0.001$

modulation, confirmed that apoptosis induced by CAPE, MG132, DOX, and VCR in PL104 cells is caspase-dependent.

Comparative apoptosis-inducing efficacy of CAPE, MG132, DOX, and VCR in bone marrow cells from leukemia patients

We evaluated morphological features of apoptosis by AO/EB staining in cells obtained from leukemia patients and PBMC from normal volunteers after 24-h exposure to each of all four drugs. In samples from patients with AML and ALL, 360 μM CAPE and 4 μM MG132 induced higher percentages of apoptosis than 5 μM VCR or 2 μM DOX in 24-h exposure assays (Fig. 9a, b). Differences were less remarkable in samples from CLL and CML (Fig. 9c).

None of the drugs tested induced a significant level of apoptosis in normal PBMC (Fig. 9d). Thus, although all four drugs appear to be selective for induction of apoptosis in leukemic cells, CAPE and MG132 exhibited a higher efficacy in AML and ALL samples.

Discussion

One of the most important advances in cancer research in recent years is the recognition that cell death, mostly by apoptosis, is crucially involved in the regulation of tumor formation and critically determines treatment response. Killing of tumor cells by most anticancer strategies currently used in clinical oncology, including chemotherapy, γ-irradiation, suicide gene therapy, and immunotherapy, has been related to activation of apoptosis signal transduction pathways such as the intrinsic and/or extrinsic pathway.

In a previous work, we showed that treatment of PL104 cells and primary leukemic cells derived from patients with CAPE, MG132, and two chemotherapeutic agents, DOX and VCR, induced morphologic hallmarks of apoptosis including cytoplasm shrinkage, chromatin condensation, and nuclear and cell fragmentation [16]. In this study, we further analyzed the apoptotic phenotype and the molecular mechanisms elicited by treatment of PL104 cells with the aforementioned drugs. By means of annexin V labeling assays, we demonstrated that CAPE, MG132, DOX, and VCR induced cell death causing exposure of PS in the outer leaflet of cell membrane, while TUNEL and DNA content assays confirmed that cell death was associated with DNA fragmentation and hypodiploid DNA content. These biochemical features are hallmarks of nuclear and extranuclear apoptosis. Thus, together with our previous morphological findings, we conclude that all four drugs induced apoptotic cell death in PL104 cells.

Proteasome inhibitors are known to induce cell death in tumor cells of different histological origin, and a number of preclinical assays have revealed their potential antitumor activity on hematological malignancies and solid tumors [24–26]. In agreement with this data, our work demonstrated that the proteasome inhibitor MG132, which is not currently included in any clinical protocol, induces apoptosis in lymphoblastoid cells PL104. CAPE was demonstrated to be cytotoxic in brain tumor cells [27], breast [13], prostate [14], and pancreas cancer cell lines [28]. However, there are few reports on CAPE effects in hematological malignancies.

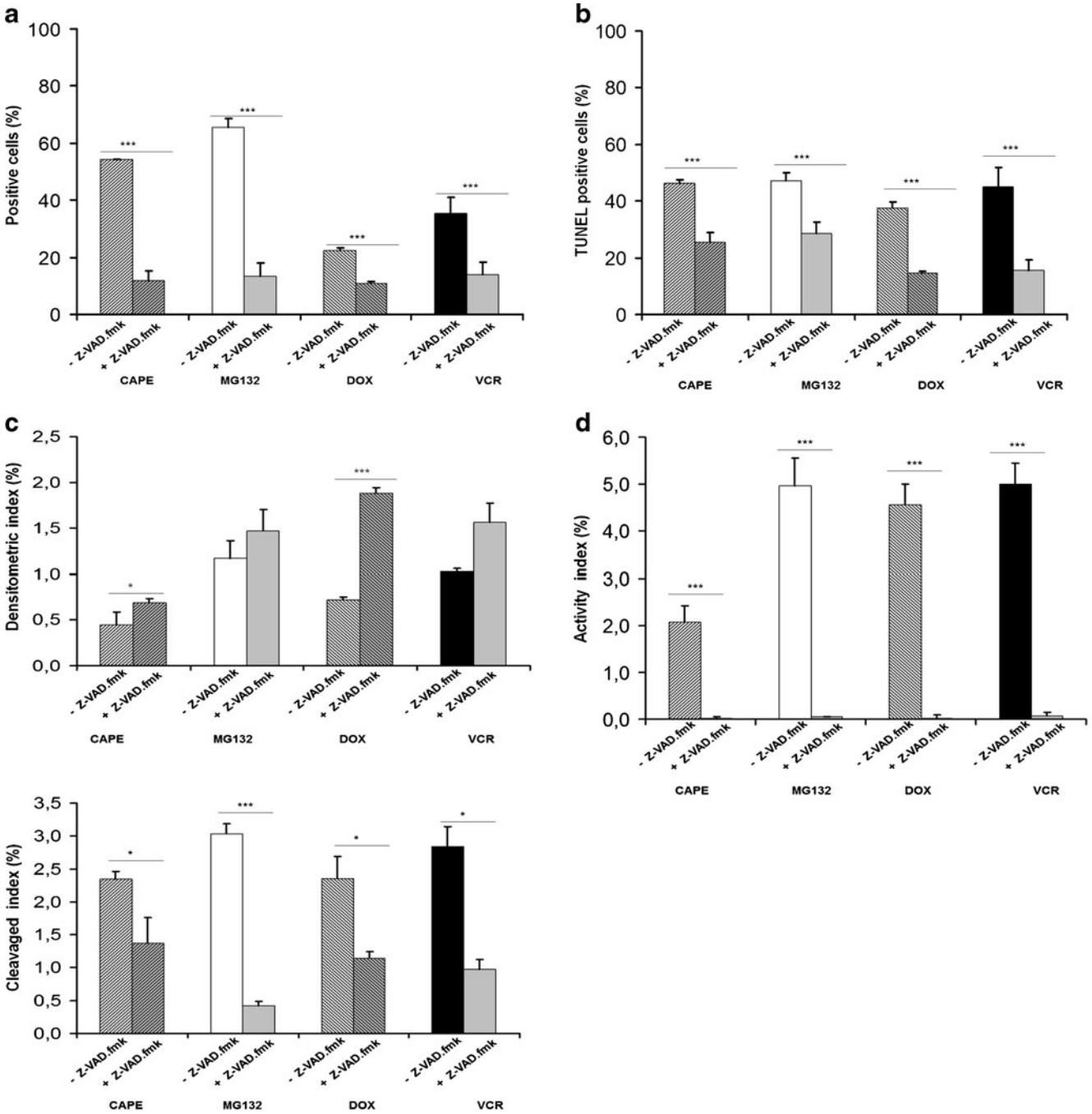

Fig. 8 Effect of pancaspase inhibitor Z-VAD.fmk on apoptotic indicators. PL104 cells were pretreated with Z-VAD.fmk 100 μM for 2 h followed by 24-h exposure to 180 μM CAPE, 2.0 μM MG132, 1.5 μM DOX, and 1.0 μM VCR. **a** Percentage of positive cells determined after AO/EB staining. **b** Percentage of TUNEL-positive cells. **c** Relative procaspase 3 and PARP expression by western blot analysis. *Bar graphs* show densitometric index (procaspase 3) or cleavage index (PARP) for the different treatments. **d** Caspase 3/7 activity by a luminescence technique. *Bar graphs* show the activity index for each case. *Bars* indicate mean value+SD of at least three independent experiments. Differences between the mean of Z-VAD.fmk-treated cells and cells treated with the corresponding drug alone were analyzed with Tukey's post-test after ANOVA; (*) $p<0.05$; (***) $p<0.001$

Thus, our finding of apoptosis induction by CAPE underscores the potential relevance of this natural product as an antileukemic drug and contributes to broaden the knowledge of its biological activity in a particular unexplored area.

We further detected drug-induced changes in the expression of Bcl-2, Bax, and survivin that are key regulatory proteins of the apoptotic program. Survivin expression was decreased by treatment with all four drugs. However, CAPE decreased survivin expression at early time points, while

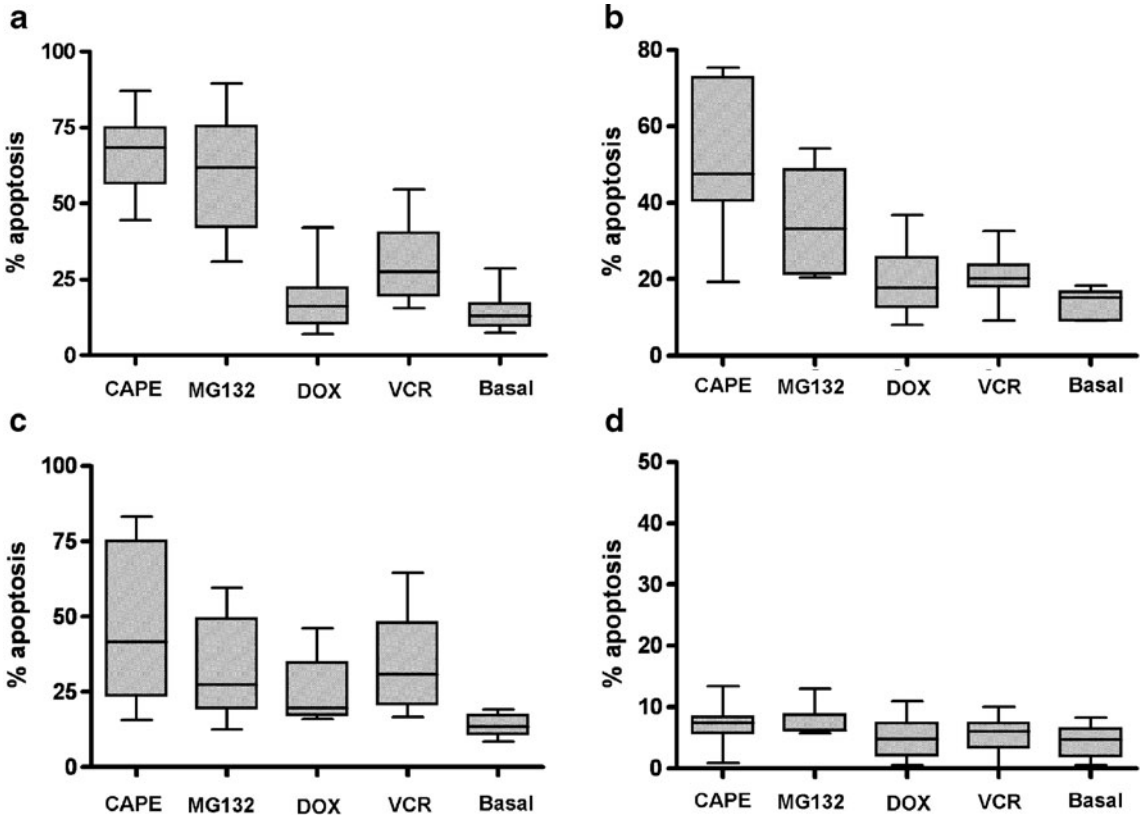

Fig. 9 Induction of apoptosis in leukemic cells and normal PBMC. *Box–whisker plots* obtained after determining the percentage of apoptotic cells by AO/EB staining, after 24-h exposure to 360 μM CAPE, 4 μM MG132, 2 μM DOX, 5 μM VCR, and nontreated cells (basal). The four sets of plots correspond to ex vivo drug-treated cells from acute myeloid leukemia patients (**a**), acute lymphoblastic leukemia patients (**b**), chronic lymphocytic leukemia together with chronic myeloid leukemia patients (**c**), and PBMC from normal healthy volunteers (**d**)

MG132, DOX, and VCR only reduced survivin after 24-h treatment. Our study is the first, as far as we are aware, to report downmodulation of survivin by CAPE. Since survivin is upregulated by a NF-κB transcription factor, decreased survivin may be due to the ability of CAPE to block NF-κB [16]. Survivin expression level changes during the different cell cycle phases and the proteasome plays a crucial role in the regulation of this temporal expression pattern. Proteasome inhibitors have been shown to stabilize survivin leading to its increased expression [29]. By contrast, our results showed that MG132 decreased survivin levels, raising the possibility that MG132 elicits a different mechanism in PL104 cells. A possible explanation could be that proteasome inhibition may lead to a massive increase in survivin expression, which in turn, results in a negative feedback mechanism that causes a considerable decrease in protein level by caspase activity.

MMP is a crucial event in triggering intrinsic apoptosis. MMP is characterized by loss of Δψm that correlates with damage of the inner mitochondrial membrane. We found that CAPE induced an early Δψm collapse, which was shown to increase at higher doses and prolonged incubation time. This result could be related to the decreased Bcl-2 expression, which in turn, may be due to the observed increased expression of Bax after treatment with CAPE. However, it could also be explained by the ability of CAPE to induce a prooxidant redox cellular state leading to Δψm collapse and initiation of apoptosis [30]. Similarly, VCR induced Δψm collapse although the effect was less dependent on the dose. Like other vinca alkaloids, VCR targets tubulin and microtubules. However, the relationship between microtubule network disturbance and the involvement of mitochondria in apoptosis is not quite evident. Even so, it has been determined that several intracellular proteins could relate inhibition of microtubules dynamic to the initiation of apoptosis [31]. Neither MG132 nor DOX induced changes in Δψm at any of the doses tested. Contrasting our results, MG132 has been shown to induce Δψm depolarization in other leukemia and hepatoblastoma cells [32, 33].

MMP causes mitochondria-to-cytosol translocation of numerous proteins that are normally confined to the intermembrane mitochondrial space. These proteins include three broad categories: direct caspase activators (e.g., cytochrome *c*), indirect caspase activators (e.g., Smac/Diablo and Omi/HtrA2), and caspase-independent cell death effectors (e.g., AIF, endonuclease G and EndoG). Thus, we evaluated the release of cytochrome *c*, Smac/DIABLO, and AIF after treatment with the drugs.

We observed a dual release of cytochrome *c* after CAPE exposure, with an early increase in the cytosolic fraction after 2 h, followed by a late increase at 24 h. Bernardi et al. described the existence of two pools of cytochrome *c*, a small one and a big one. The small pool of cytochrome *c* accounts for approximately 15 % of total protein and is tightly membrane-bound via both electrostatic and hydrophobic interactions, whereas the big one is located at the intermembrane space loosely attached as a result of weak electrostatic interactions [34, 35]. Therefore, the first peak of cytochrome *c* observed after CAPE treatment could correspond to the loosely attached pool, which once in the cytosol could induce caspase activation or increase ROS production. Both events would act as a proapoptotic feedback loop leading to a subsequent release of cytochrome *c* from the larger pool (the second peak that we observed). MG132 also induced a dual release of cytochrome *c*. In this case, the first increase in the cytosolic protein level was detected after 2 h of exposure followed by a second peak at 15 h, which was kept high up to 24 h of treatment. By contrast, DOX and VCR induced cytochrome *c* release after 6 h of treatment, which was prolonged for more than 15 h.

Only MG132 increased Smac/DIABLO expression. It is notable that once released from the mitochondria after initiation of apoptosis, Smac/DIABLO can be rapidly bound by X-linked inhibitor of apoptosis (XIAP) and directed towards the proteasome for degradation. Antiapoptotic proteins XIAP, c-IAP1, and c-IAP2 not only bind and inhibit caspases but also target proapoptotic molecules for proteasome degradation to protect cells from accidental mitochondrial damage [36, 37]. Therefore, our results support the idea that MG132 may contribute to the stabilization of proapoptotic Smac/DIABLO by preventing its proteasome degradation. It is remarkable that cytochrome *c* release occurred prior to Smac/DIABLO after treatment with MG132. This is in agreement with studies that demonstrated that Smac/DIABLO, but not cytochrome *c* efflux, is reduced when caspases are inhibited [38]. We suggest that cytochrome *c* release could act as an initial step in apoptosis of MG132-treated PL104 cells, leading to apoptosome formation and subsequent caspase activation. Caspases could, in turn, induce mitochondrial Smac/DIABLO release to the cytosol resulting in amplification of the apoptotic signal.

ROS play a critical role both on early and late steps of apoptosis. We evaluated ROS production level on PL104 cells after treatment with CAPE, MG132, DOX, and VCR. Our results showed that CAPE induced a significant increase in ROS production at early time points. Susceptibility of transformed cells to CAPE might be determined by loss of normal redox state regulation [39, 40]. Therefore, increased ROS by CAPE could have resulted from altered redox metabolic pathways and its corresponding metabolites. MG132 treatment increased ROS production in PL104 cells although not to a large extent, which contrasts results from other studies in lung tumor cells, where MG132 was shown to increase ROS production considerably [41]. DOX treatment of PL104 cells resulted in a significant increase in ROS level. DOX bioreduction, in the presence of oxygen, is known to increase ROS in cardiac cells by elevating superoxide anion levels that can be converted by superoxide dismutase to H_2O_2 and further metabolized to HO^- [42]. This fact may explain the observed DOX capacity to increase ROS while inducing apoptosis in PL104 cells. By contrast, VCR treatment showed no changes on ROS level at all doses and time points tested, suggesting that ROS is not involved in VCR-induced apoptosis mechanisms in PL104 cells.

Caspases play essential roles in apoptosis, necrosis, and inflammation. These proteases can be activated, after mitochondrial outer membrane permeabilization, and are part of the apoptotic phenotype during the execution phase more than being part of the initiation mechanism. CAPE increased procaspase 3 expression and PARP cleavage. We also observed an early increment in caspases 3/7 activity that was not followed by any morphological feature of apoptosis. This data may suggest that early activation of caspases 3/7 might be related to biochemical events unrelated to endonuclease activation. After 4 h of CAPE exposure, prior to the release of cytochrome *c* and activation of effector caspases, we observed a statistically significant increment in caspase 9 activity. MG132 treatment resulted in an increase in procaspase 3 protein expression level and a consequent increase in PARP cleavage. Using a luminescence assay, we detected a considerable increase in caspases 3/7 activity after 6–24 h of treatment and also an early and time-persistent increment of caspase 9 activity. DOX increased the expression of procaspase 3, induced PARP cleavage, and increased caspases 3/7 activity as well. Cells exposed to VCR showed an increase in PARP cleavage, but unexpectedly, no alteration on procaspase 3 expression was detected by western blot assay. Beyond these discrepancies, probably owing to differences in the activity of primary antibodies used, we confirm the ability of VCR to activate caspase 3/7 by a more sensitive technique. Neither DOX nor VCR induced significant modifications on caspase 9 activity at doses and time points tested. Pretreatment with a pancaspase inhibitor resulted in a reduction of the percentage of cells with apoptotic morphology and DNA fragmentation. It also increased procaspase 3 level with a concomitant reduction in PARP cleavage in protein extracts. Together with the absence of AIF in nuclear extract, which is an indicator of caspase-independent apoptosis, our findings support a role for caspases 3/7 in the apoptotic mechanisms elicited by all four drugs.

On the basis of the different molecular events analyzed on this work, we can conclude that CAPE and MG132

induced apoptosis of PL104 cells by eliciting the mitochondrial intrinsic pathway, whereas mechanisms of apoptosis induced by DOX and VCR may proceed through the extrinsic pathway even though definitive confirmation in this last case deserves further analysis.

An in-depth knowledge of cytotoxic mechanism elicited by CAPE and MG132 contributes to the assessment of their potential clinical efficacy. Our preliminary assessment of 20 samples obtained from leukemic patients showed that apoptosis induction by CAPE and MG132 appears to be selective for AML and ALL, at least at the experimental doses tested.

The potential of target drugs is greatly increased by an optimized combination often based upon knowledge of apoptotic-inducing mechanisms. We have previously shown that CAPE or MG132 could sensitize DOX or VCR for improved cytotoxic efficacy against PL104 cells, while the combination CAPE+MG132 had quite low cytotoxic efficacy [16].

In a more recent study, we assessed the potential of MG132 and CAPE to sensitize leukemic cells to arsenite-induced cytotoxicity and we found that MG132+arsenite were synergic in promonocytic leukemia cells, while CAPE+arsenite were antagonistic [43]. Since both CAPE and arsenite target the mitochondria and increase ROS as one of their main mechanisms, these results highlight that both in-depth mechanistic approaches and a thorough analysis of drug interaction are needed to demonstrate potential efficacy in preclinical studies [44].

We are currently assessing the induction of apoptosis ex vivo by the combination of MG132+ arsenite through these methods in bone marrow cells from patients diagnosed with myelodysplastic syndrome with the aim of validating the cytotoxic efficacy and selectivity at clinically achievable doses of arsenite and MG132. We believe that in-depth understanding of the particular molecular mechanisms of the apoptotic program elicited by novel targeted drugs contribute to rational approaches for cancer treatment.

Acknowledgments The authors thank Dr. Daniela Ureta (Servicio de Citometría de flujo, Departamento de Microbiología, Inmunología y Biotecnología, Fac. de Fcia. y Bioq., UBA, Argentina) for technical assistance and UBA and CONICET for financial support.

Conflict of interest None.

References

1. Li X, Gong J, Feldman E, Seiter K, Traganos F, Darzynkiewicz Z (1993) Apoptotic cell death during treatment of leukemias. Leukemia 7:659–670
2. Kaufmann SH, Earnshaw WC (2000) Induction of apoptosis by cancer chemotherapy. Exper Cell Res 256:42–49
3. Friesen C, Lubatschofki A, Kotzerke J, Buchmann I, Reske SN, Debatin K (2003) Beta-irradiation used for systemic radioimmunotherapy induces apoptosis and activates apoptosis pathways in leukaemia cells. Eur J Nucl Med Mol Im 30:1251–1261
4. Taraphdar AK, Roy M, Bhattacharya RK (2001) Natural products as inducers of apoptosis: implications for cancer therapy and prevention. Curr Sci 80:1387–1396
5. Milner AE, Palmer DH, Hodgkin EA, Eliopoulos AG, Knox PG, Poole CJ, Kerr DJ, Young LS (2002) Induction of apoptosis by chemotherapeutic drugs: the role of FADD in activation of caspase-8 and synergy with death receptor ligands in ovarian carcinoma cells. Cell Death Differ 9:287–300
6. Somervaille TC, Linch DC, Khwaja A (2001) Growth factor withdrawal from primary human erythroid progenitors induces apoptosis through a pathway involving glycogen synthase kinase-3 and Bax. Blood 98:1374–1381
7. Santiniab MT, Rainaldi G, Indovina PL (2000) Apoptosis, cell adhesion and the extracellular matrix in the three-dimensional growth of multicellular tumor spheroids. Oncol Hemat 36:75–87
8. Galluzzi L, Morselli E, Kepp O, Vitale I, Rigoni A, Vacchelli E, Michaud M, Zischka H, Castedo M, Kroemer G (2010) Mitochondrial gateways to cancer. Mol Aspects Med 31:1–20
9. Fesen MR, Pommier Y, Leteurtre F, Hiroguchi S, Yung J, Kohn KW (1994) Inhibition of HIV integrase by flavones, caffeic phenethyl acid and related compounds. Biochem Pharmacol 48:595–608
10. Bankova V, Christov R, Kujumgiev A, Marcucci MC, Popov S (1995) Chemical composition and antibacterial activity of Brazilian propolis. Z Naturforsch [C] 50:167–172
11. Breger J, Fuchs BB, Aperis G, Moy TI, Ausubel FM, Mylonakis E (2007) Antifungal chemical compounds identified using a *C. elegans* pathogenicity assay. PLoS Pathog 3:168–178
12. Orsolic N, Sver L, Terzic S, Tadic Z, Basic L (2003) Inhibitory effect of water-soluble derivatives of propolis and its polyphenolic compounds on tumor growth and metastasizing ability: a possible mode of antitumor action. Nut Cancer 47:156–163
13. Watabe M, Hishikawa K, Takayanagi A, Shimizu N, Nakaki T (2004) Caffeic acid phenethyl ester induces apoptosis by inhibition of NFκB and activation of Fas in human breast cancer MCF–7 cells. J Biol Chem 279:6017–6026
14. Mc Eleny K, Coffrey R, Morrissey C, Fitzapatrick JM, Watson WG (2004) Caffeic acid phenethyl ester-induced PC–3 cell apoptosis is caspase–dependent and mediated through the loss of inhibitors of apoptosis proteins. BJU Int 94:402–406
15. Xiang D, Wong D, He Y, Xie J, Zhong Z, Liz Z, Xie J (2006) Caffeic acid phenethyl ester induces growth arrest and apoptosis of colon cancer cells via the [beta]-catenin/T-cell factor signaling. Anti-Cancer Drugs 17:753–762
16. Cavaliere V, Papademetrio D, Lorenzetti M, Valva P, Preciado MV, Larripa I, Monreal MB, Pardo ML, Hajos SE, Blanco G, Álvarez E (2009) CAPE and MG–132 have apoptotic and antiproliferative effects on leukemic cells but not on normal mononuclear cells. Trans Oncol 2:46–58
17. Ha J, Choi HS, Lee Y, Lee ZH, Kim HH (2009) Caffeic acid phenethyl ester inhibits osteoclastogenesis by suppressing NF–κB and down-regulating NFATc1 and c–Fos. Int Immunopharmacol 9:774–780
18. Yuan BZ, Chapman JA, Reynolds ST (2008) Proteasome Inhibitor MG132 induces apoptosis and inhibits invasion of human malignant pleural mesothelioma cells. Transl Oncol 1:129–140
19. Letoha T, Somlaia C, Taka'csb T, Szabolcsb A, Rakonczay ZJ, Ja'rmayb K, Szalontaic T, Vargad I, Kaszakie J, Borosf I, Dudaf E, Hacklerg L, Kuruczh I, Penkea B (2005) The proteasome inhibitor MG132 protects against acute pancreatitis. Free Radical Biol Med 39:1142–1151
20. Ustundag Y, Bronk SF, Gores GJ (2007) Proteasome inhibition-induces endoplasmic reticulum dysfunction and cell death of human cholangiocarcinoma cells. World J Gastroenterol 13:851–857

21. Xingming D, Fengqin G, Stratford May WG (2003) Bcl2 retards G1/S cell cycle transition by regulating intracellular ROS. Blood 102:3179–3185
22. Alaniz L, García MG, Cabrera P, Arnaiz M, Cavaliere V, Blanco G, Álvarez E, Hajos S (2004) Modulation of matrix metalloproteinase-9 activity by hyaluronan is dependent on NF-κB activity in lymphoma cell lines with dissimilar invasive behavior. Biochem Biophys Res Commun 324:736–743
23. Bustamante J, Caldas Lopes E, Garcia M, Di Libero E, Álvarez E, Hajos SE (2004) Disruption of mitochondrial membrane potential during apoptosis induced by PSC 833 and CsA in multidrug resistant lymphoid leukemia. Toxicol Appl Pharmacol 199:44–51
24. Adams J (2004) The development of proteasome inhibitors as anticancer drugs. Cancer Cell 5:417–421
25. Naujokat C, Sezer O, Zinke H, Leclere A, Hauptmann S, Possinger K (2000) Proteasome inhibitors induce caspase–dependent apoptosis and accumulation of 21WAF1/Cip1 in human immature leukemic cells. Eur J Haematol 65:221–236
26. Li W, Zhang X, Olumi AF (2007) MG-132 sensitizes TRAIL-resistant prostate cancer cells by activating c-Fos/c-Jun heterodimers and repressing c-FLIP(L). Cancer Res 67:2247–2252
27. Lin YH, Chiu JH, Tseng EWS, Wong TT, Chiou ESH, Yen ESH (2006) Antiproliferation and radiosensitization of caffeic acid phenethyl ester on human medulloblastoma cells. Cancer Chemother Pharmacol 57:525–532
28. Chen MJ, Chang WH, Lin CC, Liu CY, Wang TE, Chu CH, Shih SC, Chen YJ (2008) Caffeic acid phenethyl ester induces apoptosis of human pancreatic cancer cells involving caspase and mitochondrial dysfunction. Pancreatology 8:566–576
29. Zhao J, Tenev T, Martins LM, Downward J, Lemoine NR (2000) The ubiquitin–proteasome pathway; regulates survivin degradation in a cell cycle–dependent manner. J Cell Sci 13:4363–4371
30. Kirkland RA, Franklin JL (2001) Evidence for redox regulation of cytochrome *C* release during programmed neuronal death: antioxidant effects of protein synthesis and caspase inhibition. Neurosci 21:1949–1963
31. Estéve MA, Carré M, Braguer D (2007) Microtubules in apoptosis induction: are they necessary? Curr Cancer Drug Targets 7:713–729
32. Zanotto-Filho A, Delgado-Cañedo A, Schröder R, Becker M, Klamt, Moreira JC (2010) The pharmacological Nfkappa B inhibitors BAY117082 and MG132 induce cell arrest and apoptosis in leukemia cells through ROS–mitochondria pathway activation. Cancer Lett 288:192–203
33. Emanuele S, Calvaruso G, Lauricella M, Giuliano M, Bellavia G, D'Anneo A, Vento R, Tesoriere G (2002) Apoptosis induced in hepatoblastoma HepG2 cells by the proteasome inhibitor MG132 is associated with hydrogen peroxide production, expression of Bcl-XS and activation of caspase 3. Int J Oncol 21:857–865
34. Bernardi P, Scorrano L, Colonna R, Petronilli N, Di Lisa F (1999) Mitochondria and cell death. Eur J Biochem 264:687–701
35. Garrido C, Galluzzi L, Brunet M, Puig PE, Didelot C, Kroemer G (2006) Mechanisms of cytochrome *c* release from mitochondria. Cell Death and Differ 13:1423–1433
36. Nagy K, Szekely-Szuts K, Izeradjene K, Douglas L, Tillman M, Barti-Juhasz H, Dominici M, Spano C, Luca CG, Conte P (2006) Proteasome inhibitors sensitize colon carcinoma cells to TRAIL–induced apoptosis via enhanced release of Smac/DIABLO from the mitochondria. Pathol Oncol Res 12:133–142
37. MacFarlane M, Merrison W, Bratton SB, Cohen GM (2002) Proteasome mediated degradation of Smac during apoptosis: XIAP promotes Smac ubiquitination in vitro. J Biol Chem 277:36611–36616
38. Adrain C, Creagh EM, Martin SJ (2001) Apoptosis–associated release of Smac/DIABLO from mitochondria requires active caspases and is blocked by Bcl–2. EMBO 20:6627–6636
39. Chiao C, Carothers AM, Grunberger D, Solomon G, Preston GA, Carl Barrett J (1995) Apoptosis and altered redox state induced by caffeic acid phenethyl ester (CAPE) in transformed rat fibroblast cells. Cancer Res 55:3576–3583
40. Kudugunti SK, Vad NM, Ekogbo E, Moridani MY (2009) Efficacy of caffeic acid phenethyl ester (CAPE) in skin B16–F0 melanoma tumor bearing C57BL/6 mice. Invest New Drugs 29:52–62
41. Han YH, Park WH (2010) MG-132 as a proteasome inhibitor induces cell growth inhibition and cell death in A549 lung cancer cells via influencing reactive oxygen species and GSH level. Hum Exp Toxicol 29:607–614
42. Shi R, Huang CC, Aronstam RS, Ercal N, Martin A, Huang YW (2009) *N*–acetylcysteine amide decreases oxidative stress but not cell death induced by doxorubicin in H9c2 cardiomyocytes. BMP Pharmacol 9:7
43. Lombardo T, Cavaliere V, Costantino SN, Kornblihtt L, Alvarez EM, Blanco GA (2012) Synergism between arsenite and proteasome inhibitor MG132 over cell death in myeloid leukaemic cells U937 and the induction of low levels of intracellular superoxide anion. Toxicol Appl Pharmacol 258:351–366
44. Lombardo T, Anaya L, Kornblihtt L, Blanco G (2012) Median effect dose and combination index analysis of cytotoxic drugs using flow cytometry. Intech Open Publisher Rijeka, Croatia, pp 393–418